Striped-Pattern Deterioration and Morphological Analysis of Injection Molding Comprising Polypropylene/Ethylene–α-Olefin Rubber Blends. II. Influence of Heating

Koki Hirano,[1,2] Satoshi Tamura,[1] Yutaka Obata,[3] Toshitaka Kanai[2,3]

[1]*Research & Development Division, Prime Polymer Company, Limited, 580-30 Nagaura, Sodegaura-City, Chiba 299-025, Japan*
[2]*Division of Material Sciences, Graduate School of Natural Science & Technology, Kanazawa University, Kakuma-Machi, Kanazawa-City, Ishikawa 920-1192, Japan*
[3]*Research & Development Laboratory, Idemitsu Kosan Company, Limited, Anasaki-Kaigan, Ichihara-City, Chiba 299-0193, Japan*

Received 12 July 2007; accepted 30 September 2007
DOI 10.1002/app.27403
Published online 21 December 2007 in Wiley InterScience (www.interscience.wiley.com).

ABSTRACT: Unique deterioration with a striped pattern caused by thermal heating is reported for injection molding comprising polypropylene/ethylene–α-olefin rubber blends. This stripe is due to the formation of glossy and cloudy parts in alternation approximately perpendicular to the flow direction of the molten resin. On the surface of the cloudy part, a number of micro-objects appear. They have a dome shape about 10 μm in diameter and 2 μm height. Some experimental evidence indicates that the objects are composed of the rubber contained in the blends. On the other hand, only a few objects appear in the glossy region after heating. This is the reason that the stripe with the micro-objects (migrating rubber to the surface) is examined in terms of a higher order structure of injection molding with laser scanning microscopy, wide-angle X-ray scattering, and microhardness (Martens hardness). Consequently, we have concluded that this thermally deteriorated stripe depends on periodic changes in the crystallinity along the flow direction. The evidence indicates that a snakelike flow occurs during the injection process of the molding. © 2007 Wiley Periodicals, Inc. J Appl Polym Sci 108: 76–84, 2008

Key words: blends; injection molding; morphology; poly (propylene) (PP); rubber

INTRODUCTION

Polypropylene (PP) is one of the most widely used resins in the industrial field; its applications include not only commodity equipment, packages, films, and home electric appliances but also automotive parts.[1,2] PP is easily modified by blending with rubber[3–7] and talc[8,9] to obtain higher performance for impact strength, rigidity, and dimensional stability, especially in automotive parts[10] such as bumper faces and instrument panel garnish. In the last 2 decades, PP/rubber blends have become the main materials for these automotive parts for which the surface finishing is required to be as good as the mechanical properties.

In general, these parts are manufactured by the injection-molding method. For injection molding comprising PP/rubber blends, it is well known that a periodically striped mark called a tiger stripe or flow mark occurs on the surface of the injection molding from the gate side to the flow end and is just about perpendicular to the flow direction of the molten resin.[11–14] This stripe is due to the formation of glossy and cloudy parts in alternation. A severe tiger stripe sometimes spoils the surface finish of paintless or partially painted parts. Some previous studies, using numerical simulation[12] and/or visualization,[15] have reported the induction process of the tiger stripe, in which an unstable flow of the molten resin, like a snake moving, is the origin of the tiger stripe. Moreover, the shape of the dispersed rubber domain controls the stripe.[11,14] The orientation of the domain near the surface of the molding is higher (elongated along the flow direction) in the glossy part in comparison with the one for the cloudy part of the tiger stripe. In our previous article,[14] we reported that the stripe can become inconspicuous by a reduction of the rubber orientation through the control of the base impact-type PP design, including the molecular weight distribution of the homo-PP portion and intrinsic viscosity of the rubber portion of the PP. Therefore, the tiger stripe defect does not become a severe issue for real automotive parts

Correspondence to: K. Hirano (koki.hirano@primepolymer.co.jp).

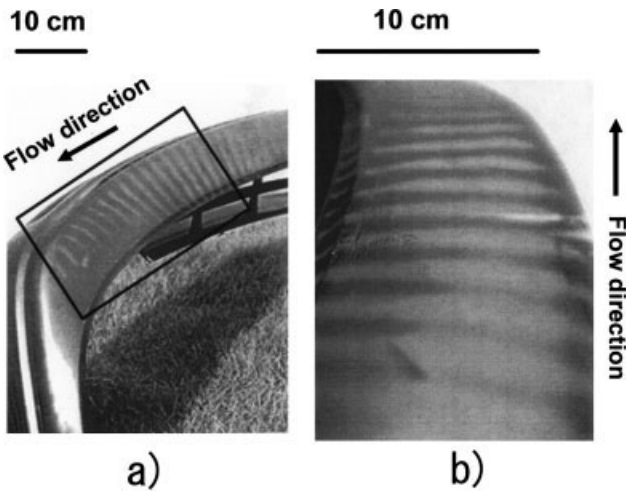

Figure 1 Model bumper exposed outdoors for a year.

because of appropriate designs controlling how inconspicuous the stripes are.[13,14,16]

Even though the tiger stripe is inconspicuous when the bumper is assembled to an automotive body, outdoor exposure during the real use of the automotive for several years or more causes severe striped deterioration. Figure 1 shows typical striped-pattern deterioration of an injected bumper comprising a PP/rubber blend with talc as the inorganic filler after exposure for 1 year on Okinawa Island in southern Japan. A striped pattern due to the formation of strongly and weakly whitened parts in alternation can be easily seen by the naked eye. The tiger stripe was not severe like this just after the molding (the initial state for the exposure). However, both sunlight and exposed environments induced severe deterioration in the tiger stripe pattern. In this sample, the glossy (darkish) and cloudy (whitish) parts of the original tiger stripe became weakly and strongly whitened parts, respectively. Here, this striped-pattern deterioration was paid special attention because it became a serious defect in the surface finishing design. Thus, striped deterioration is important in the application of PP/rubber blends for real use. There have been quite a few studies regarding this phenomenon already. In other studies, we have discussed the influence of UV irradiation on the striped deterioration of a PP/rubber model blend not containing carbon black (CB).[17] There, UV irradiation provided striped deterioration formed by microvoids that occurred under the surface of the molding. The density of the microvoids alternated along the flow direction of the molten resin during the injection process; the difference of the density changed approximately periodically along the direction and formed the deteriorated stripe macroscopically. Surprisingly, the microvoid was generated just inside the dispersed rubber domain.[17]

Following the article already mentioned,[17] we studied the influence of heating on striped deterioration. As described in the Results and Discussion section, a simple heat treatment led to severe macroscopic striped deterioration visible to the naked eye. However, the microscopic origin of this deteriorated stripe was quite different from that for the case of UV irradiation.

EXPERIMENTAL

Materials

The PP used in this study was a high-impact copolymer with a 50 g/10 min melt flow rate (at 230°C and 2.16 kg), a 7 wt % concentration of the rubber component (propylene–ethylene copolymer) as the *p*-xylene-soluble portion, and a 98% mesopentad fraction (mmmm) for its homo-PP portion. It was catalyzed with a Ziegler–Natta catalyst system (the fourth generation: $TiCl_4$/internal donor/electron donor/$MgCl_2$). Prime Polymer Co., Ltd. (Tokyo, Japan), manufactured the PP; it is named bPP here because it was used as the base PP in this study. The ethylene–α-olefin rubber was a metallocene-catalyzed ethylene–butene rubber (EBR) named A-1050 (melt index = 1.2 g/10 min at 190°C, density = 0.87 g/cm^3) that was manufactured by Mitsui Chemical, Inc. (Tokyo, Japan). The talc (JM-209), having a 4-μm average diameter according to the laser diffraction method, was supplied by Asada Mineral Co., Ltd. (Tokyo, Japan). Table I shows the material formulations of the PP blends used in this study.

Sample preparation

The blends were prepared with a 2FCM twin-screw compounding mixer (barrel diameter = 2 in.) from KOBE Steel, Ltd. (Hyogo, Japan); it was set at a barrel temperature of 200°C and a screw speed of 900 rpm. The productivity was 50 kg/h. The antioxidant agent Irganox 1010 (1000 ppm; Ciba Specialty Chemicals, Basel, Switzerland) was added to the blends to prevent thermal degradation during this compounding process. These blends were molded with an IS200°CN injection machine (Toshiba Machine Co., Ltd., Shizuoka, Japan), the clamping force of which was 200 tons. The operating conditions were set at a

TABLE I
Formulation of the Blends Used in This Study

	bPP	BL-1	BL-2	BL3
bPP	100	70	63	63
EBR	—	30	27	27
Talc	—	—	10	10
CB	—	—	—	0.6

TABLE II
Results of Thermal Heating on the Surface Appearance of the Plate

	bPP	BL-1	BL-2	BL-3
Before heat treatment	No stripe	No stripe	Inconspicuous stripe (tiger stripe)	Inconspicuous stripe (tiger stripe)
After heat treatment	No stripe	Conspicuous stripe	Conspicuous stripe	Conspicuous stripe

Annealing conditions: 140°C and 240 h.

cylinder temperature of 220°C and a filling time of 3.5 s. The specimen shape was a plate 420 mm long, 100 mm wide, and 3 mm thick.

Heat treatment

The injection plate was left in an oven. A Perfect oven, produced by Tabai Espec Corp. (Osaka, Japan), was used at a given temperature.

Confocal laser scanning microscopy (LSM)

An LSM-GM microscope (Olympus Corp., Tokyo, Japan) was operated under the following conditions: 20× magnification and 0.32 mm × 0.48 mm view. Both the brightness and surface roughness used here were obtained by an analysis of the reflected light from the surface.

Wide-angle X-ray diffraction scattering (WAXS)

The degree of crystallinity was calculated with WAXS. The WAXS analysis was based on the Ruland method.[18] X-ray diffraction profiles were obtained by a camera system connected to an imaging plate (IPR-420, Bruker AXS K.K., Ibaragi, Japan) using graphite-monochromatized Cu Kα radiation (0.1542 nm) from an X-ray generator (Ultra-X 18, Rigaku Co., Ltd., Tokyo, Japan). The distance from the sample to the detector was 90 mm. The diffraction patterns were measured at the parts from 10–30- and 80–110-μm depths from the surface for the injection plate with and without the heating. The specimens for WAXS were carefully sliced off parallel to the machine direction (i.e., flow direction of the molten resin during the injection molding)/transverse direction by a 10-μm step with a sliding microtome (LS-113, Yamato Kouki Industrial Co., Ltd., Saitama, Japan).

Microhardness of the surface

An ENT-1100a apparatus (Elionix, Inc., Tokyo, Japan) measured the Martens hardness (a microhardness method) according to ISO 14577.

RESULTS AND DISCUSSION

Stripe pattern caused by thermal heating dependent on the material formulation

As reported in our previous article,[14] tiger stripes strongly depend on the material formulation; an increase in the contents of both the blended rubber and talc tends to make the tiger stripe conspicuous. In addition, CB rolling as a UV absorber suppresses the induction of the deteriorated stripe caused by UV irradiation. Therefore, the influence of the material formulation should first be confirmed in a thermal heating exposure experiment. These results are summarized in Table II. Before heat treatment, the bPP and BL-1 (PP/rubber binary blend) samples showed no tiger stripe on their surface because the induction distance of the tiger stripe was long enough for the flow length of the molding plate. On the other hand, the other samples, BL-2 (PP/rubber/talc) and BL-3 (PP/rubber/talc/CB), showed inconspicuous tiger stripes on the side edge of the injection molding approximately perpendicular to the flow direction of the molten resin. It is thought that the blended talc made the induction distance of the tiger stripe shorter near the gate of the injection molding.[13]

After the heating, all the samples except bPP showed a conspicuous striped pattern on the surface. These stripes could be easily seen by the naked eye. These results show that the striped deterioration is caused by not only UV irradiation but also a given condition of thermal heating. Moreover, it is important that simple thermal heating could cause striped deterioration to a sample containing CB. As we reported in our latest article,[17] UV irradiation could not cause any striped deterioration in the blend to which CB was added because of the role of CB as a UV absorber. Thus, the striped deterioration noted by us is very unique, and it is interesting to study the phenomenon and its mechanisms. Figure 2 shows the striped deterioration caused by the heating for BL-3. In this photograph, the striped deterioration is easy for readers to recognize. A similar stripe occurred for samples BL-1 and BL-2 (see Table II). However, these two samples did not contain CB and were a whitish, natural color. Because of strong reflecting light, we could not take a good photograph to demonstrate the stripe for these natural-

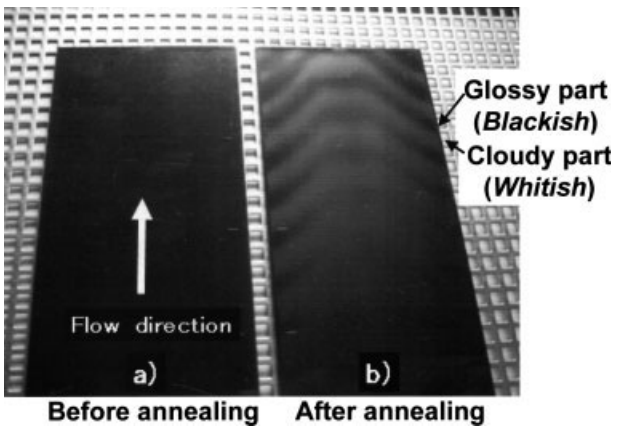

Figure 2 Conspicuous stripe caused after the heating (140°C, 240 h).

colored samples. However, we will define the glossy and cloudy parts of the stripe here. They were high-gloss and low-gloss parts, respectively, adjacent to each other along the stripe. In addition, the cloudy part is recognized as a whitish part by the naked eye in comparison with the glossy part. For simplification, those parts of the original sample (not annealed) corresponding to the glossy and cloudy parts caused by heating are also called glossy and cloudy parts, respectively.

Surface observation along the stripe with LSM

LSM observation was performed to analyze the change in the striped surface caused by the thermal heating. All the specimens that presented the stripe with the heat treatment were analyzed. A set of LSM photographs of the striped surface of BL-1 is shown in Figure 3. In the case of the original plate (without heat treatment), a smooth surface was observed for both parts corresponding to the glossy parts after this heat treatment. On the other hand, quite a different morphology was obtained for the parts with the heat treatment. This result indicates an interesting phenomenon: simple thermal heating caused a dramatic change in the surface morphology for the cloudy parts of the deteriorated stripe but not for the glossy parts. A number of dark-colored objects having an approximately circular shape appeared on the surface of the cloudy part. However, only a few of the objects appeared on the surface of the glossy part. Thus, this deteriorated stripe is controlled by the density of the objects on a microscopic scale. The same results were obtained for other samples with the deteriorated stripe (BL-2 and BL-3).

These objects are entirely darkish colored but are bright in the center of the circular shape in the LSM image (Fig. 3). According to the principle of LSM, this object has a three-dimensional shape with a rounded surface. Figure 4 shows a side view of the object with its spatial dimensions from LSM. It should be noted that the scales are different for the diameter and height. These data show that the object has a dome shape approximately 10 μm in diameter and 2 μm height.

A change in the surface roughness before and after the heat treatment is shown in Figure 5. Here, a series of glossy and cloudy parts along the flow direction of the molten resin were measured; the odd and even numbers correspond to the glossy and cloudy parts, respectively. For the original plate (before the heat treatment), the surface roughness is an almost constant value of about 0.2 μm that is independent of both parts. The smooth surface shown in Figure 3 explains this result. On the other hand, the roughness strongly depends on the striped plate (after the heat treatment). That is, although the

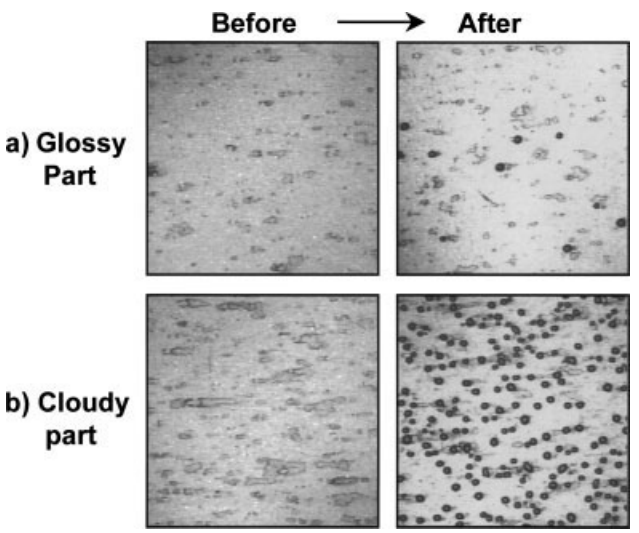

Figure 3 Surface observation of BL-1 with LSM.

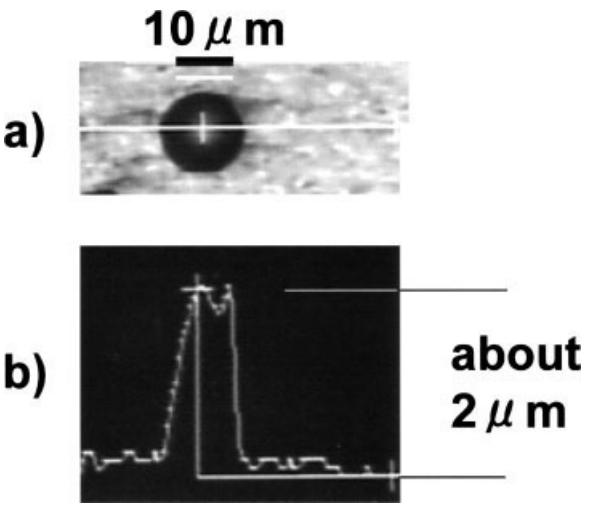

Figure 4 Dimensions of an object on the surface with LSM: (a) upper view and (b) side view.

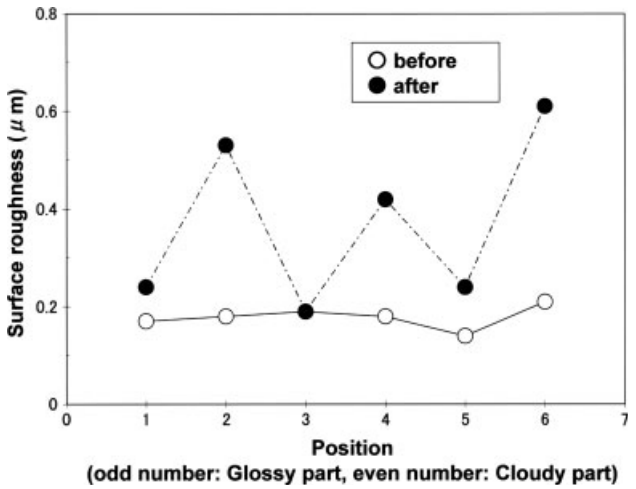

Figure 5 Surface roughness for the glossy and cloudy parts on the stripe.

glossy parts have roughness similar to that of the original plate (ca. 0.2 μm), that of the cloudy parts clearly increased up to about 0.4–0.6 μm after the heat treatment. In this case, the existence of many objects simply explains that the roughness increased. Many objects occurring on the surface diffuse incident light, so the part attains low gloss, which the naked eye recognizes as a cloudy part.

Thus, it has been confirmed that the stripe caused by the heat treatment is controlled by the differences in the surfaced roughness due to the density of the dome-shaped objects.

Characterization of the dome-shaped objects

To discuss the mechanism of the striped deterioration caused by the heat treatment, it is very important to determine what the component of the dome-shaped objects is. Therefore, some analytical methods were carried out to characterize the objects. We concluded that the objects are the rubber component contained in the blends on the basis of the following results:

1. These dome-shaped objects indicated elasticity when they were picked by a needle during optical microscopy observation at room temperature. The only component having elasticity used in this study was rubber.
2. It was found that solvent washing with *p*-xylene at room temperature made these dome-shaped objects disappear from the surface of the annealed plate. Moreover, it was noteworthy that the conspicuous stripe caused after heating also disappeared with this solvent washing. In general, *p*-xylene at room temperature can dissolve nonvulcanized olefinic rubber, which includes the EBR used here but not crystalline homo-PP. This result shows that the dome-shaped objects consist of the olefinic rubber component of the blends.
3. As Figure 4 shows, the object has a curvy surface like a dome or hemisphere. This means that surface tension was dominant in forming the shape of the object. That is, the component was in a liquidlike state when the object was formed at the heating temperature of 140°C. The EBR used here has a melting point of 40°C at the peak temperature (reported by the manufacturer). This indicates that the heating temperature is high enough to place the EBR in a liquidlike state. Of course, PP does not melt at this temperature because of its melting point of about 163°C.

In addition, it was clear that the additives, antioxidation agent, and so forth did not form the object. Certainly, the additives can bleed from the inside to the surface in injection molding, but they are not elastic. Also, ethanol can remove the additives through wiping. We tried to wipe the heated plate that had the dome-shaped objects with ethanol; however, they remained even after wiping.

A spectroscopic method (Fourier transform infrared spectroscopy) was also used to determine the components of the objects, but it was not successful. Similar spectra based on the methylene bonds of the main-chain backbone of both PP and EBR made it difficult to classify them.

Difference in the higher order structures for the striped parts

Clearly, the rubber component forming the dome-shaped objects bleeds out from the inside of the plate to the surface after the heat treatment. We are interested in how and why the dome-shaped rubber appears on the surface after the heat treatment. Moreover, the density of a number of the objects was quite different between the glossy and cloudy parts. Also, the objects appeared evenly spread apart from each other (15–20 mm) on the same molding (see Figs. 2 and 3).

Incidentally, we have paid attention to the difference in the higher order structures between the surfaces with and without the migrating rubber in terms of the rubber content and crystallinity. If a region corresponding to the cloudy part has a higher content of rubber, it must tend to generate more blisters consisting of the dome-shaped rubber object after the heat treatment because of static probability. Also, if the crystallinity is lower at the region corresponding to the cloudy part, the dispersed rubber domain must tend to move from the inside to the surface through the amorphous region.

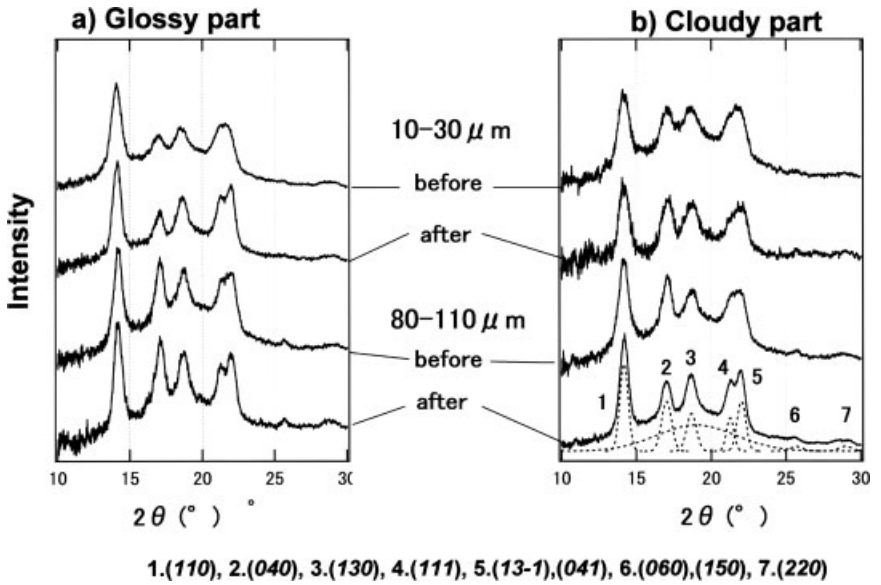

Figure 6 Depth dependence of WAXS for BL-1 before and after the heat treatment.

To clarify the differences, WAXS was measured to obtain crystallinity depending on the depth. Figure 6 shows WAXS patterns for the depths of 10–30 and 80–110 μm for the glossy and cloudy parts before and after the heat treatment. The crystallinity obtained by the decomposed peaks based on the α form is summarized in Table III and also shown in Figure 7 (a simple average depth was adopted for the abscissa axis).

The crystallinity after heating is constant (almost 52%) and does not depend on either the parts or the depths.

The condition of the heat treatment (140°C, 240 h) is enough to saturate the crystallinity of PP in the blends.

It is important that the crystallinity is almost 52% for all the specimens after the heat treatment. That is, the rubber content is quite constant in all the parts of the plate, including both the glossy and cloudy parts of this thermally deteriorated stripe. The cloudy part with a high density of the dome-shaped migrating rubber does not have a high concentration of the rubber locally in comparison with that for the glossy part with fewer migrating rubbers. As a result, the rubber content does not control the generation of migrating rubber in this case. Moreover, as we reported in our previous article,[14] the rubber content is constant along the flow direction in this sample in terms of an image analysis based on scanning electron microscopy photographs (BL-1 is the same sample as sample B in that article).

The crystallinity before the heat treatment is of interest. The crystallinity at the depth of 10–30 μm (20 μm on average) for the cloudy part before the treatment is 35 wt % (indicated by an arrow in Fig. 7). On the other hand, the other parts have a constant crystallinity of about 43 wt % independent of the

TABLE III
Crystallinity (wt %) Obtained with WAXS of the Shallow Region of BL-1 Before and After Heating

	Depth (μm)	Crystallinity (%)	
		Glossy part	Cloudy part
Before heat treatment	10–30	42	35
	80–110	43	44
After heat treatment	10–30	52	50
	80–110	52	52

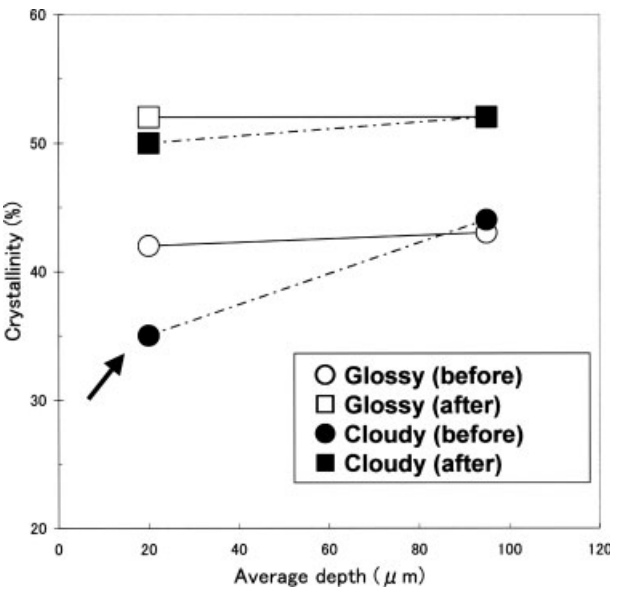

Figure 7 Crystallinity dependence on the depth before and after the heating.

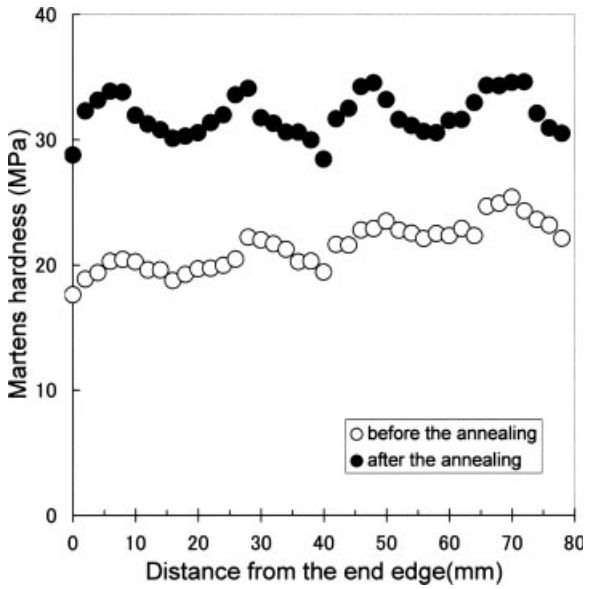

Figure 8 Martens hardness (microhardness) of the surface for BL-1 before and after the heating (indentation force = 20 mN).

position and depth. This result suggests that the shallower region near the surface of the cloudy part has low crystallinity in comparison with that of the glossy part when the plate is molded by the injection-molding method.

To obtain more information on how the depth is controlled by the crystallinity, the microhardness test named Martens hardness was performed. These data were obtained at a selective condition for the maximum test force of 20 mN, and the balance of effective range and error was taken into account. Figure 8 shows the microhardness profiles along the flow direction of the molten resin for BL-1 before and after the heat treatment. The origin of the abscissa axis is 0 mm and corresponds to the flow end of the plates.

It should be noted that periodical wavelike patterns repeating at the top and bottom of the hardness clearly appear for the data before and after the heat treatment. Here, the positions of the top and bottom perfectly matched for the plates before and after the treatment. Of course, the positions of the top and bottom correspond to the glossy and cloudy parts, respectively. Under this condition for the load of 20 mN, the maximum indentation depths were about 5 μm. In general, 10 times the maximum indentation depth should be considered empirically to discuss microhardness.[19] Therefore, the depth of about 50 μm from the surface was considered in this experiment on the basis of this empirical rule. Then, the average depth was simply calculated to be 25 μm. It is close to the average depth of 20 μm for the WAXS measurement for the shallower region near the surface. Thus, we found that the glossy part and cloudy part before the heat treatment (just a molding plate) have high and low hardness corresponding to high and low crystallinity, respectively, in the shallower region of 10–30 μm.

It was confirmed that the difference of the microhardness depends on the crystallinity in the shallow region.

After the heat treatment, the microhardness rose with increasing crystallinity. However, the profile kept a periodical pattern. The gap between the top and bottom is larger than that before the heat treatment, even though the crystallinity is constant at about 52 wt % for both the glossy and cloudy parts. It was estimated that the dome-shaped rubbers that occurred on the surface reduced the hardness because the surface morphology strongly contributed to the microhardness on the basis of this principle.

Estimation of the difference in the crystallinity along the flow direction

We have already reported on the morphology of the dispersed rubber phase in sample BL-1.[17] In that report, BL-1 is named sample C. Here, only the result is cited for the discussion.

Highly oriented rubber domains exist in a shallow region from the surface. Under this zone, weakly oriented rubber domains exist. In the glossy part and cloudy part, the zone having highly oriented rubber domains is thick (ca. 50–60 μm) and thin (ca. 20–30 μm), respectively. The difference in the rubber orientation is controlled by the unstable flow, which resembles a moving snake, near the flow-end edge during the filling process of injection molding.

Michaeli et al.[20] reported that the orientation of the dispersed rubber domains accompanies the molecular orientation of the PP matrix in PP/rubber blends. In addition, it is well known that the molecular orientation of crystalline PP easily crystallizes itself on the basis of an entropy-loss effect.

In the cloudy part before the heat treatment, the zone in which the rubber domains are highly oriented is thin. That is, the molecular orientation of PP is also low in this region. This explains why the cloudy part has low crystallinity in its shallow region.

Mechanism of the striped deterioration with the rubber migration of the surface

We will discuss the mechanism by which the dome-shaped rubber migrations selectively occur in the cloudy parts. The stripe formed by the heat treatment can be seen immediately after the treatment. That is, the migrating rubber moves from the inside to the surface at this high temperature. The melting point of the added rubber (EBR) is below 40°C.

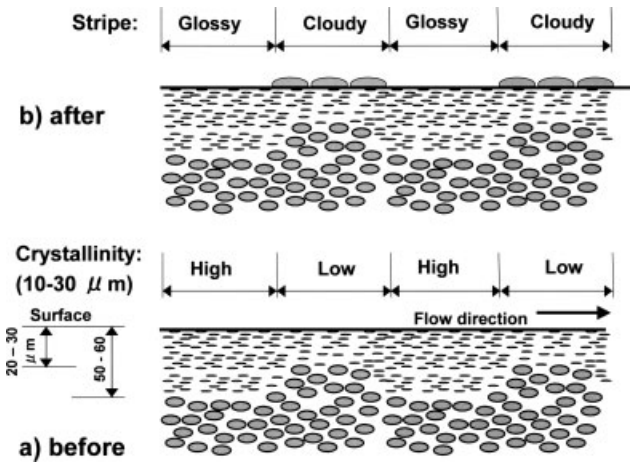

Figure 9 Schematic drawing of the striped deterioration of the PP/rubber binary blend (a) before and (b) after the heat treatment (with a conspicuous stripe). Gray-colored portions indicate the rubber components, including dispersed rubbers and bleeding rubbers.

Therefore, the rubber flows easily during the heat treatment because of its low viscosity at the experimental temperature of 140°C. The crystallinity increases by isothermal crystallization during the heat treatment. The change in the crystallinity indicates the largest value of 15% point (50% − 35%) for the shallow region (10–30 μm) of the cloudy part, which has been calculated with the data shown in Table III. For the glossy part, the change is 10% point (52% − 42%) for the same region of the depth. With increasing crystallinity, the specific volume of the matrix PP decreases. This volume reduction probably becomes an effective force to control migration of the rubber component from the inside to the surface on the basis of such a squeezing effect. However, it seems to be hard to completely explain the difference in the numbers of the migrating rubbers between the glossy and cloudy parts in terms of the squeezing effect; the migrating rubbers are concentrated on the surface of the cloudy part (see Fig. 3). As already mentioned, the orientation of the matrix PP is regarded as lower in the cloudy part than in the glossy part. Therefore, it is possible that a crystalline network is loose in the cloudy part. We suppose that the migration of rubber can easily pass through this loose crystalline network. On the other hand, a compact crystalline network with the molecular orientation of PP prevents the migration of the rubber. To clarify this mechanism, further information will be discussed.

Incidentally, it is a fact that the rubbers migrate from the inside to the surface. A typical migrating rubber is about 10 μm in diameter and 2 μm high (Fig. 4). It is much larger than the size of the dispersed rubber domain in the shallow region near the surface. The average diameters of the long axis of the domain were measured to be 2.9 and 3.9 μm in the machine direction (i.e., flow direction)/normal direction cross section for the cloudy and glossy parts, respectively. It seems that these small domains move through the poor network of the crystalline matrix PP because of migration supported by the squeeze effect, and they aggregate mutually on the surface of the plate during the heat treatment. The rubber is in a liquidlike state at the temperature of 140°C. Thus, these aggregated rubbers form a curvy shape based on the surface tension, and finally the dome-shaped migration rubbers occur.

A conceptual schematic obtained in this study is shown in Figure 9.

CONCLUSIONS

In this article, we have reported unique deterioration with a striped pattern caused by heat treatment for injection molding comprising PP/rubber binary components.

The striped deterioration has been discussed in terms of higher order structures involving the morphology of the dispersed rubber, crystallinity of the PP matrix, and so forth.

The obtained results can be summarized as follows:

1. A simple heat treatment can cause striped deterioration on an injection molding composed of PP/rubber blends, the glossy and cloudy parts repeating alternately.
2. The deteriorated stripe consists of dome-shaped objects occurring on the surface of the cloudy part.
3. The dome-shaped objects are the rubber component contained in the blends.
4. The cloudy parts, having many migrations, indicate low crystallinity before the heat treatment.
5. A squeeze effect with reduction of the specific volume after the heat treatment seems to be a force to migrate the rubber.

The authors are grateful to A. Torikai and H. Nakatani for their suggestion of this study. M. Ando supported the Martens hardness analysis. Finally, Prime Polymer Co., Ltd., is acknowledged for permitting the release of this study.

References

1. Moore, E. P. Polypropylene Handbook; Hanser Gardner: Cincinnati, 1996.
2. Polypropylene: An A to Z Reference; Karger-Kocsis, J., Ed.; Kfslmer Academic: Dordrecht, The Netherlands, 1999.
3. Liang, J. Z.; Li, R. K. Y. J Appl Polym Sci 2002, 77, 409.

4. D'Orazio, L.; Marcarella, C.; Martuscelli, E.; Polato, F. Polymer 1991, 32, 1186.
5. van der Wal, A.; Nijihof, R.; Gaymans, R. J. Polymer 1999, 40, 6031.
6. Walton, K. L. Rubber Chem Technol 1996, 77, 3523.
7. Wu, G.; Nishida, K.; Takagi, K.; Sano, H.; Yui, H. Polymer 2005, 45, 3085.
8. Obata, Y.; Sumitomo, T.; Ijitsu, T.; Matsuda, M.; Nomura, T. Polym Eng Sci 2001, 41, 408.
9. Maiti, S. N.; Sharma, K. K. J Mater Sci 1991, 27, 4605.
10. Maxwell, J. Plastics in the Automotive Industry; Woodhead: Cambridge, England, 1994.
11. Patham, B.; Papworth, P.; Jayaraman, K.; Shu, C.; Wolkowicz, M. D. J Appl Polym Sci 2005, 96, 423.
12. Grillet, A. M.; Bogaerds, A. C. B.; Peters, G. W. M.; Baaijens, F. P. T. J Rheol 2002, 46, 651.
13. Hirano, K. Idemitsu Tech Rep 2005, 48, 124.
14. Hirano, K.; Suetsugu, Y.; Kanai, T. J Appl Polym Sci 2007, 104, 192.
15. Yokoi, H.; Narita; J. Polymer Processing Society Asia/Australia Meeting; Polymer Processing Society: New York, 1999; p 143.
16. Nakagawa, M.; Hirano, K.; Obata, Y.; Sugita, Y.; Nomura, T.; Matsuda, M.; Iwai, H.; Nagai, T. U.S. Pat. 6,667,359 (2003).
17. Hirano, K.; Tamura, S.; Kanai, T. J Appl Polym Sci 2007, 105, 2416.
18. Stein, R. S.; Rhodes, M. B. J Appl Phys 1960, 31, 1873.
19. Samuels, L. E.; Mulhearn, T. O. J Mech Phys Solids 1965, 5, 125.
20. Michaeli, W.; Cremer, M.; Bluhm, R. Kunststoffe 1993, 83, 992.